Pergamon

PII: S0042-6989(97)00027-8

Vision Res., Vol. 37, No. 16, pp. 2195–2206, 1997

Printed in Great Britain
0042-6989/97 $17.00 + 0.00

2D Motion Aliasing Yielding 3D Ambiguity. A Study with Variants of a Necker Cube

ANDREI GOREA,*† CHRISTEL AGONIE*

Received 4 August 1995; in revised form 19 January 1996; in final form 21 January 1997

The 2D projection of a rotating Necker cube yields an ambiguous 3D interpretation based on both 2D shape and kinetic depth information. The present study shows that the alternation rate of the two 3D interpretations is constant with the rotation speed up to some critical value (around 25 turns/min for a cube whose sides subtend 2.5 deg) and increases monotonically thereafter. It is proposed that the additional perceptual reversals (PRs) observed at high rotation speeds are due to the increased frequency of the crossovers of the cube's edges. These crossovers yield 2D motion "aliasing" (or discontinuity) and "veridical" (or continuity) motion components. The motion aliasing (or crossover) hypothesis states that, in addition to the inherent ambiguity of the dynamic 2D projection of 3D objects, perceptual motion/perspective reversals will occur any time the discontinuity speed takes over the continuity speed. It is proposed that the relative strengths of the two components depend on the linear speed of the projected edges and that the discontinuity components take over the continuity one in the speed range where contrast sensitivity (or, above threshold, efficiency) is a decreasing function of speed. The motion aliasing hypothesis was tested and supported in a series of independent experiments showing that, for rotation speeds higher than 25 turns/min the PR rate increases with the crossover frequency at a constant speed, with linear speed at a constant crossover frequency and with the similarity of the crossing bars in terms of their orientation, polarity and spatial overlap. In addition, some of these experiments suggest that 2D shape and kinetic depth 3D-cues combine in such a way that the average PR rate they yield together is the same as the PR rate yielded by each of them independently. In the Discussion section we elaborate on issues related to the perceptual combination of ambiguous shape and kinetic depth, 3D cues. © 1997 Elsevier Science Ltd.

3D shape Kinetic depth effect Motion aliasing

INTRODUCTION

Among the many figures yielding perceptual bi- (or multiple-) stability, the Necker cube has probably generated most of the experimental studies (see Kruse & Stadler, 1995). As a general rule, studies of this kind focused on the nature (stochastic, chaotic or deterministic) of these processes and on their underlying neural mechanisms. For the particular case of the Necker cube, perceptual reversals (PRs) were assessed with both static and rotating figures. The use of rotating cubes has the potential advantage of rendering the observer's decision as to the occurrence of a PR more objective. The spontaneous perspective reversal yielded by such figures is concomitant with (equivalent to/consubstantial with) a reversal in the perceived direction of rotation: naïve observers do not discriminate between the two and typically trust that they are reacting to physical changes.

A static and a rotating Necker cube do not, however, necessarily address the same perceptual processes. To achieve this, one should

1. demonstrate that the rate and distribution of the PRs do not depend on the rotation speed and
2. consider that the perceptual ambiguity yielded by a rotating cube resides both in the ambiguity of its spatial configuration and of its associated optic flow (kinetic depth effect—KDE).

In this paper we will address experimentally only the effect of rotation speed upon the rate and temporal distribution of PRs.‡ We will offer a theoretical interpretation of the observed effect and test that interpretation by means of a number of independent experiments. In the Discussion section we will expand on the issue of the dual ambiguity source yielded by a rotating Necker cube.

*Laboratoire de Psychologie Expérimentale, René Descartes University and C.N.R.S., 28 rue Serpente, 75006 Paris, France.
†To whom all correspondence should be addressed.

‡While anecdotal reports of an observed dependency of the PR rate on rotation speed might have been exchanged among psychophysicists (Share Blackburn, Univ. of New South Wales, Sidney, personal communication), we do not know of any published paper or conference abstract on this topic.

EXPERIMENT 1: PRS AS A FUNCTION OF ROTATION SPEED

The data reported in this section are part of a more comprehensive study on the temporal structure of PRs as a function of the rotation speed in the presence of physical reversals. In that study, the rotation direction was physically reversed in the range of 0–24 reversals per minute and this rate was randomized across sessions. Here we report only on the data obtained during inspection periods without such physical reversals. It is worth mentioning, however, that the PR rates and interval distributions did not depend on the presence of physical reversals.

Method

Stimuli, procedure and observers. The Necker cube was presented in orthographic projection on the screen of a Silicon Graphics Iris 4D-35 workstation. Each side of the cube subtended 2.5 deg at an inspection distance of 1 m. The cube was built out of dark bars 0.9′ thick displayed on a 20 cd/m^2 yellow background. Three elevation projection angles were used: 15, 30 and 45 deg. The cube was animated so as to rotate around a vertical axis crossing its centre which was marked by a black fixation dot. The rotation speeds were 1, 3, 8, 25 and 72 turns/min. Two additional speeds (40 and 60 turns/min) were used in a control experiment (see below).

One session consisted of a 1-min inspection period characterized by the projection angle, the rotation speed (and the number of physical reversals—see above). The starting 3D position of the cube was randomized over sessions. There were eight naïve observers instructed to press a button any time they perceived a reversal of the direction of rotation. They were asked to maintain fixation the best they could and were encouraged to respond as rapidly as possible.* The observers were naïve in the sense that they were not aware (until told) that their PRs were not caused by physical reversals and, as a corollary, that they did not discriminate between perceptual and physical reversals. The order of the experimental conditions was randomized across observers. There were altogether 45 sessions (i.e., 45 min of observation) per observer, including the sessions yielding a variable number of physical reversals (not presented here). There were breaks varying from 30 sec to 5 min between sessions. The data presented below include the PRs observed during sessions void of physical reversals together with the PRs recorded before any physical reversal in sessions including such physical reversals.

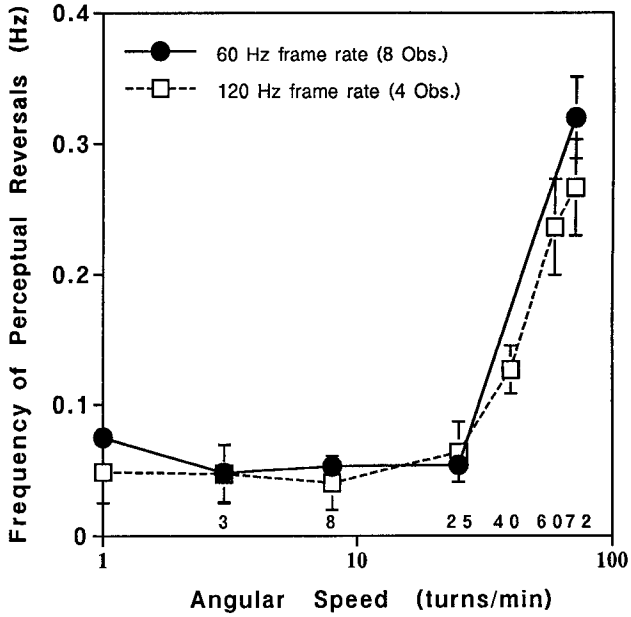

FIGURE 1. Perceptual reversal (PR) rate for a rotating Necker cube as a function of its angular speed (note the log abscissa). Circles are PR rates averaged over eight observers run with an animation frame rate of 60 Hz. Squares are PR rates averaged over four observers run with an animation frame rate of 120 Hz. Vertical bars are ±1 SE.

Because of the low frame rate of the SGI workstation (60 Hz), visible motion aliasing occurs at fast rotation speeds (here 72 turns/min). As an answer to the concern of one reviewer that such aliasing may account for the main effect we report below, the experiment was run once again under the same experimental conditions (with only one, 15 deg elevation angle), while taking advantage of the stereo presentation capacity of the SGI station which allows an animation at 120 Hz frame rate. (This manipulation halves the vertical resolution of the screen and thus decreases the luminance of the stimuli. We have no reason to believe that such an effect has any bearing on the phenomena described in this study.) These data were obtained from four additional, naïve observers.

Results

The rate of PRs did not depend on the elevation angle of the orthographic projection. The data obtained under these three conditions were grouped together to yield 3 min of inspection per rotation speed and per observer. The results averaged across the eight (and the additional four) observers are shown in Fig. 1. Circles and squares show PR rates obtained for animations using frame rates of 60 and 120 Hz, respectively. The main observation is that the PR rate is constant with rotation speed up to about 25 turns/min (slightly less for the 120 Hz animation rate) and increases monotonically thereafter (by a factor of about 5 at 72 turns/min). Whilst the PR rate for speeds slower or equal to ≈25 turns/min is well within the range of the reversal rates reported in the literature for

*To ensure that eye movements were not involved in the reported speed-related effects (e.g. Flamm & Bergum, 1977; Gale & Findlay, 1983; Sabrin & Kertesz, 1983), we ran two quick, informal experiments with a slowly rotating cube (8 t/min): (1) four observers were asked to freely move their eyes around the fixation point while pressing a response knob for each PR; (2) the same observers fixated the rotating cube which was also jittered around its centre at a range of frequencies and amplitudes. Neither of these conditions yielded a significant increase in the PR rate.

stationary and slowly rotating cubes (about 0.07 PRs/sec, i.e., 4.2 PRs/min)*, the drastic increase of this rate at 72 turns/min (20 reversals/min) is significantly out of this range. The literature does not provide any theoretical hint to account for this phenomenon.

An analysis of the time-interval histograms cumulated over the eight observers for slow (1–25 turns/min) and for fast speeds (72 turns/min) confirms the speed-related effect described above. When fit with gamma-like functions (see also Maloney & Gorea, 1995; Agonie, 1996), these distributions yield a mean and a median time interval of 10.4 and 7.7 sec for the slow speeds and 2.9 and 2.3 sec for the fast speed, i.e., a factor of approx. 3.5 shorter. Thus, once again, for some unknown reason, fast rotations yield significantly shorter time intervals between PRs than slow rotations.

THE CROSSOVER HYPOTHESIS

Nothing in particular occurs with the perceived spatial structure of the cube within the speed range used in this experiment. To account for the speed dependence of the PR rate, one must then investigate phenomena which are not phenomenologically obvious. Initially, we envisaged a "cognitive" interpretation of this effect (see Koffka, 1935, pp. 285–303). Given that the bars of which the Necker cube is built are all alike, we considered the possibility that, at some particular instants, some of them can be confounded perceptually. In particular, this would be the case with the vertical bars when they cross over: when two vertical bars are superimposed during a rotation cycle, they transiently lose their "identity". Loss of the two bars' "identity" amounts to mislabelling their 2D direction of drift so that the rightward moving bar is "confounded" with the leftward drifting bar and vice versa. As a consequence, the observer will perceive a reversal of the direction of rotation and, concomitantly, a perspective reversal.

The fact is that the notions of "identity" and "confusion" do not have an objective psychophysical status. In addition, they do not explain why the putative "identity loss" is not progressive and abruptly starts for speeds above 25 turns/min. An *ad hoc* threshold device triggered by rotation speeds higher than this arbitrary limit has no obvious sensory significance. The notions of "identity" and "confusion", however, can be rendered psychophysically tractable if one considers the 2D motion structure of a pair of bars crossing over. Figure 2 illustrates this structure within a space–time system of coordinates for a continuous motion case.

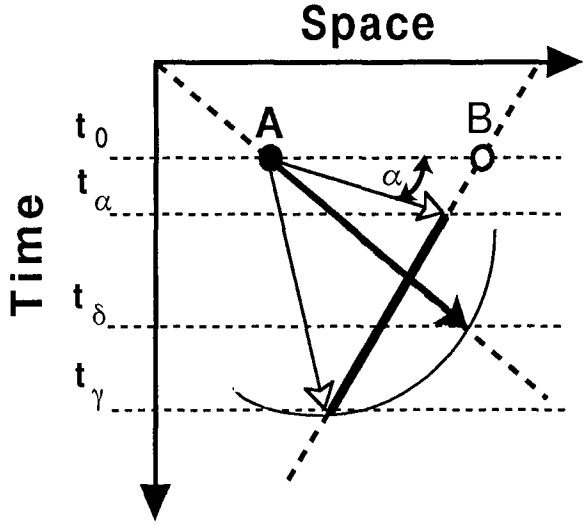

FIGURE 2. Space–time diagrams of two continuously drifting dots (or bars) crossing-over. Possible spatio-temporal matches of the drifting objects A and B are shown both before and after their crossover. The space–time trajectories of these two objects are shown by the heavy dashed lines. Horizontal dashed lines are critical points in time. The heavy vector on the trajectory of object A (from $\mathbf{t}_0$ to $\mathbf{t}_\delta$) shows the continuity motion component; its length is related to the critical sampling rate (i.e., the maximum spatio-temporal jump). The two thin vectors are discontinuity components delimiting the interaction range between A and B and thereby the range of discontinuity components (the heavy line superimposed on B's trajectory between the endpoints of these vectors). The length of the short discontinuity vector (from $\mathbf{t}_0$ to $\mathbf{t}_\alpha$) is limited by angle α which specifies the maximum visible speed (given the spatial structure of A and B). The length of the second discontinuity vector (from $\mathbf{t}_0$ to $\mathbf{t}_\gamma$) is made here equal to that of the continuity vector on the (false) assumption that the minimum allowed spatio-temporal sampling rate is independent of speed (the arc of the circle centred on A).

The heavy dashed lines in Fig. 2 show the spatio-temporal paths of objects A and B and they will be hereafter referred to as the continuity speeds. To generalize, the two objects are shown to drift at different speeds (i.e., the angles of the heavy dashed lines). Insofar as objects A and B are identical, they can, in principle, cross-match at any point of space–time so that object A will eventually follow object B's trajectory and vice versa, thus yielding the perception of a motion reversal. Such a transient cross- or mismatch may occur both before and after their crossover; it will be hereafter referred to as the discontinuity speed. Note that all discontinuity speeds before the crossover are faster than the continuity speed, whereas they are all slower after the crossover. In practice, the interaction range (i.e., where a mismatch may occur—the heavy line superimposed on the B-trajectory) will be limited by the highest (angle α) and lowest visible discontinuity speeds (thin vectors with open arrows). In turn, these limiting visible discontinuity speeds will depend on a number of factors, of which three are briefly discussed below.†

*The literature also reports that PR rate typically increases over time and may reach, for highly "trained" observers, up to 30 reversals/min (Maloney & Gorea, 1995).

†Other factors are: (i) The probability with which a discontinuity speed takes over a continuity speed as a function of their relative sensitivities (see also the following footnote). (ii) The spatio-temporal sampling rate (given by the length of the continuity and discontinuity vectors in Fig. 2) beyond which sampled motion introduces visible spurious motion components (Watson & Ahumada, 1983). In turn, the limiting spatio-temporal sampling rate will depend on (iii) the size (or spatial frequency content); (iv) the animation rate; and (v) the contrast of the moving objects (for a recent review of these issues see Todd & Norman, 1995). In Fig. 2, the limiting sampling rate factor is ignored and the endpoints of both the continuity and discontinuity vectors lie on a circle with the origin at $A-t_0$.

The relevance of the above observations is revealed when one considers the spatio-temporal integration of drifting stimuli by the underlying motion detectors, the space–time orientation selectivity of these sensors and the characteristic contrast sensitivity function of speed. When, because of a transient spatio-temporal mismatch, the motion sensor optimally responding to the continuity component is replaced by the sensor optimally responding to the discontinuity component, the latter only starts integrating the spatio-temporally oriented energy, whilst the former might have already reached its integration limit (around 100 msec according to McKee & Welch, 1985). Moreover, the length of the drift trajectory being inversely correlated with the spread of the spatio-temporal orientation spectrum, the longer the motion trajectory, the less the noise in the motion sensors responding to the continuity vector. As a consequence, whereas the system may well be more sensitive to the discontinuity than to the continuity speeds, the additional energy integrated along the continuity trajectory and the less noisy responses of the continuity motion sensor yielded by longer trajectories could reverse the effect of this sensitivity ratio.

Sensitivity functions of speed (measured with periodic—Kelly, 1979—or truncated periodic stimuli—Burr & Ross, 1982) are band-pass with a shallow low-speed and a steep high-speed branch. When measured with thin, drifting bars like those used in the present experiments, contrast sensitivity is a low-pass function of speed with a corner speed around 1 deg/sec (Agonie, 1996). At suprathreshold levels (as used in this study), perceived contrast is also a low-pass function of speed (e.g., Georgeson & Sullivan, 1975; Kulikowski, 1976).

Taken together, the three observations above provide an explanation of why the discontinuity components take over the continuity one only beyond some critical speed. For as long as the range of continuity and discontinuity speeds lies within the flat region of effective contrast function of speed, these components will all yield equal activities within the subserving motion sensors. However, because the continuity vector always has the advantage of a larger spatio-temporal integration range, it will take over the discontinuity components (both slower and faster) and no motion aliasing will occur. The situation is different for speeds where the effective contrast (and/or sensitivity) starts decreasing. In this speed range, the motion detectors sensitive to the slower discontinuity speeds will be more activated than those responding to the (faster) continuity speed and will thus yield motion aliasing with an increasing probability.* This phenomenon will then translate into additional PRs of the rotating cube. However, because the longer drift trajectory benefits only the continuity vector, the speed at which PRs will start increasing should occur at a velocity (to be specified) higher than the corner velocity.

A quantitative test of this motion aliasing hypothesis would initially require a quantitative specification of all the factors determining the interaction range of two drifting objects (see Fig. 2 and footnotes on previous page). This is beyond the scope of the present paper. Instead, the remainder provides a series of four (among other possible†) qualitative tests addressing the general form of this hypothesis, namely the relationship between the PR rate and the frequency of the crossover events at low and high speeds.

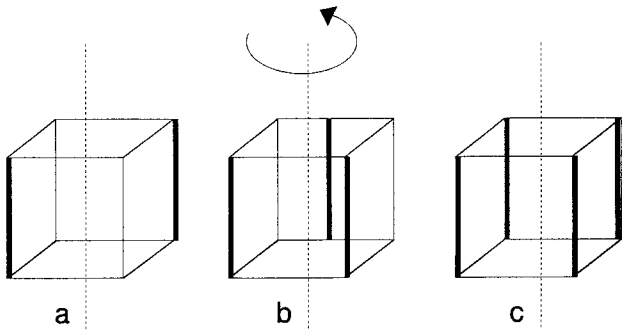

FIGURE 3. Illustration of the three stimulus configurations used in Experiment 2: (a) two bars corresponding to the edges describing a diagonal plane through the Necker cube; (b) three bars, two of which delimit one of the Necker cube's faces and a third bar placed at the midpoint of its parallel surface; (c) four bars displayed as the vertical edges of the cube. All configurations rotated around a vertical axis passing through the centre of the virtual cube.

EXPERIMENT 2: PRS AS A FUNCTION OF ROTATION SPEED AND OF THE NUMBER OF VISIBLE ROTATING BARS

If, for speeds faster than ≈25 turns/min, the PRs are critically dependent on the number of crossovers (per time unit), it is expected that they will also depend on the number of rotating bars. In the rotating Necker cube used here, the most critical crossovers are yielded by its four vertical bars. If this number is reduced, the number of crossovers will be reduced proportionally and so should the number of PRs. Experiment 2 tests this idea.

Method

Stimuli, procedure and observers. The stimuli consisted of orthographic projections of two, three and four vertical bars rotating in 3D. The 2- and 4-bar configurations were subsets of the actual Necker cube projected

*We do not know of any study having assessed the precise relationship between the relative sensitivity to two (or more) mutually exclusive interpretations of an ambiguous figure (such as, for example, a counterphase grating; see Gorea & Lorenceau, 1984) and the probability that one of them takes over the other. Pending further investigations, we simply go along with the qualitative conjecture that the two are positively correlated.

†The nature of our interpretation requires that the additional PRs have a periodic structure matched to the temporal periodicity of the crossovers in the rotating stimulus. We have tried to reveal this periodicity both in the Fourier spectrum of the observed PRs and in their autocorrelation function. However, the relatively reduced number of PRs observed for the total of 3 min of inspection period per observer and the fact that these 3 min were, in fact, partitioned in periods of 1 min each, yielded very noisy Fourier spectra with more than one dominant energy peak at frequencies difficult to localize. We, therefore, abandoned this line of analysis.

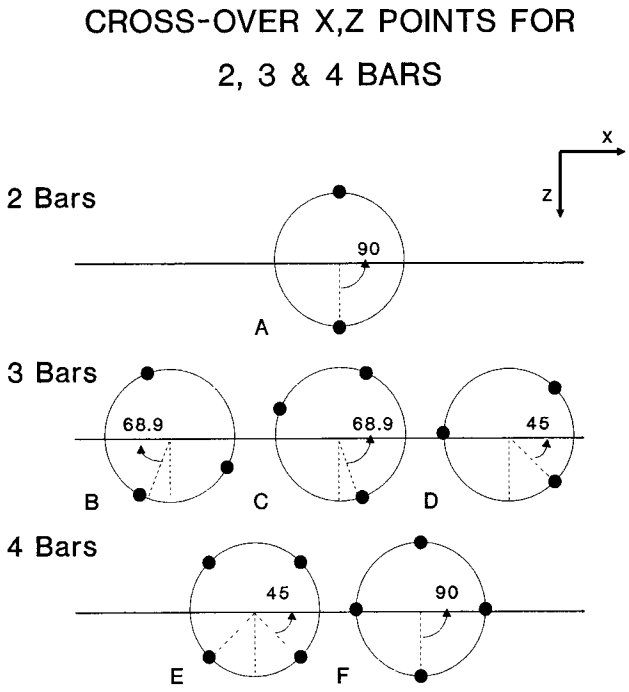

FIGURE 4. The crossover points of the three configurations of Fig. 3 shown in the x,z plane. The crossovers occur at 90 deg for the 2-bar configuration (A), at ± 68.9 deg and 45 deg for the 3-bar configuration (B, C and D) and at ± 45 and 90 deg, for the 4-bar configuration (E and F).

orthographically with an elevation angle of 15 deg. The two vertical bars corresponded to the edges on a diagonal plane through the cube; the four bars were the four vertical edges of the cube. In the 3-bar configuration, two bars represented the edges of one surface of the cube while the third bar was placed at the midpoint of the parallel surface. Figure 3 illustrates the three configurations.

All configurations rotated around a vertical axis passing through the centre of the virtual cube. The angular speed could be 25, 30, 40, 50, 60 and 72 turns/min. One experimental session was 1 min long and was characterized by the stimulus configuration (two, three or four bars) and by the rotation speed. Each experimental session was repeated three times in an order randomized across the five naïve observers, none of whom participated in Experiment 1. As before, the observers were asked to press a button any time they experienced a PR. They had no problem perceiving a 3D structure, even for the 2-bar configuration. This was not the case when the two bars were presented (in a control experiment) with a null elevation angle and with a constant (as opposed to a sinusoidally modulated) linear speed.

Figure 4 displays the 2-, 3- and 4-bar stimuli projected on the x–z plane at the crossover points. With respect to the plane of fixation (shown by the horizontal line in each panel), the crossovers occur at 90 deg for the 2-bar stimulus (A), at 68.9 deg (B, C) and 45 deg (D) for the 3-bar stimuli and at 45 (E) and 90 deg (F) for the 4-bar stimuli. There are two, six and eight crossovers/turn for the 2-, 3- and 4-bar configurations, respectively. However, in 50% of cases, the 4-bar configuration presents two crossovers at the same time (at + and −45 deg; E) which, if counted as such, yield twelve (instead of eight) crossovers/turn. For the 3-bar configuration, whenever two of the bars cross over (B, C, D) and their depth "identity" is lost, the third bar remains unambiguously in its currently perceived depth plane and may well disambiguate the whole configuration. This is not the case with the 4-bar configuration where, when two bars cross over (F), the remaining two bars lying in the zero-depth plane cannot bias the current 3D percept one way or another. In case (E), the possibility exists that only one of the two simultaneous crossovers entails motion aliasing. The PR yielded by this motion aliasing will then be counteracted by the second crossover where the continuity velocity has taken over. All these considera-

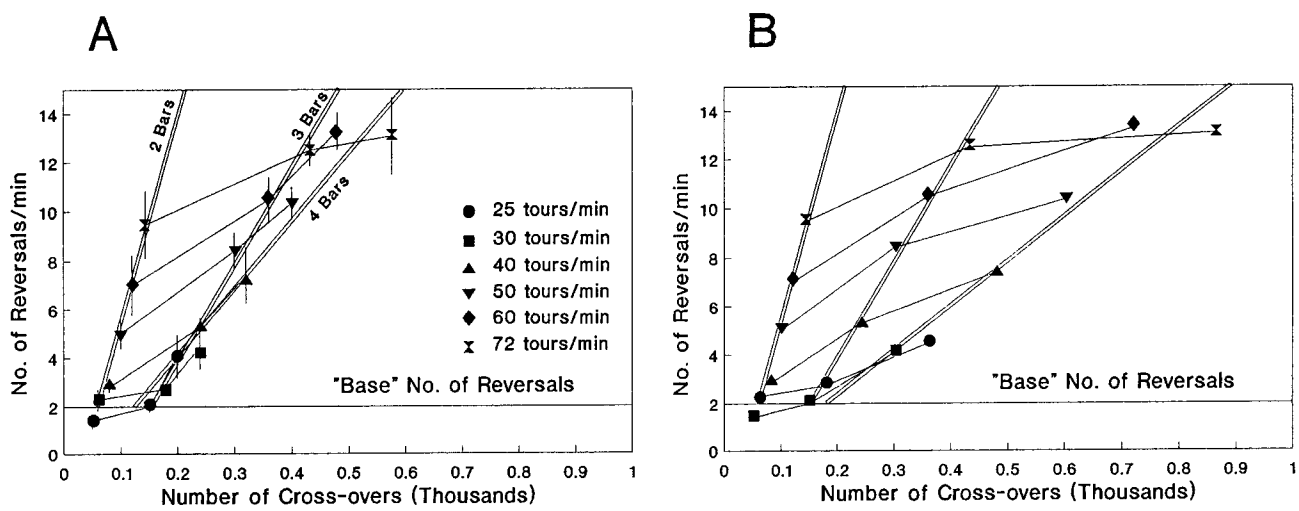

FIGURE 5. PR rate as a function of the number of crossovers per minute for six angular speeds (different symbols connected by straight lines; see inset). Straight double-lines are linear regressions computed across PR rates yielded by the six speeds for the three stimulus configurations (i.e., 2-, 3- and 4-bars). Horizontal lines refer to the average PR rate obtained with angular speeds equal to and slower than 25 turns/min. Vertical bars are ± 1 SE. (A) and (B) differ only in the way the number of crossovers was computed for the 4-bar stimulus, namely 8 or 12 per turn (see text for further details).

tions make the precise effect of the number of crossovers on the PR rate difficult to predict. At least, the "crossover" hypothesis predicts a monotone increase of the PR rate with the number of visible rotating bars (i.e., with the number of crossovers per rotation cycle).

Results and discussion

Figure 5 presents the number of PRs/min averaged across the five observers as a function of the number of crossovers computed for each of the three stimulus configurations (i.e., 2-, 3- and 4-bars). Given the uncertainty concerning the "effective" number of crossovers per turn for the 4-bar stimulus, Fig. 5 displays the data collected under this condition when this effective number is taken to be 8 [Fig. 5(A)] and 12 [Fig. 5(B); see Methods].

In Fig. 5, different symbols refer to different angular speeds (see inset). Identical symbols (i.e., constant speed) are connected by straight lines. Double lines are linear regressions computed across PR rates yielded by the six angular speeds for each of the three stimulus conditions. The horizontal line shows the average number of PRs obtained with the complete Necker cube in Experiment 1 for speeds up to 25 turns/min: these are the conditions where, presumably, the crossovers are not effective in eliciting a PR. Vertical bars show ± 1 standard error.

The data display the following main characteristics.

1. For any given speed, the number of PRs increases with the number of crossovers, and thus with the number of bars (connected symbols).
2. For a given stimulus configuration (1-, 2- and 3-bars), the number of PRs also increases with the number of crossovers, and thus with the angular and linear speed (double-lines). Both observations are in qualitative accord with the "crossover" hypothesis.
3. As a consequence of (1) and (2), one also notes that, for a given number of crossovers (a vertical slice in either of the two panels), the number of PRs increases with speed and decreases with the number of bars.

The linear relationship between PRs and speed for the 4-bar condition represents a better fit to the data when the number of crossovers is computed on a basis of 12 rather than 8 crossovers/turn (see the Methods section; this observation might indicate that the former computation is a better estimate of the number of "effective" crossovers). In any case, the number of PRs tends to saturate above 12–14 (in this case, above approx. 600 crossovers/min). Within the speed range used here, speed *per se* does not seem to yield such a saturation effect. Finally, one observes that the number of PRs tends asymptotically to the "baseline", namely in the speed range where, in accordance with the "crossover" hypothesis, the crossovers are not effective in eliciting PRs.

In the above account of the data, the only observation which cannot be directly related to the "crossover" hypothesis is the negative correlation (at a constant number of crossovers) between PRs and the number of bars: this hypothesis requires that the number of PRs be constant when the speed and the number of crossovers are constant. Why then do the three double-lines in Fig. 5 not overlap?

The answer may arise from the observation that equal angular speeds for the three (2-, 3- and 4-bars) stimulus configurations do not represent equal linear speeds. The "crossover" hypothesis predicts that, at a fixed number of crossovers per time unit, the PR rate should be a unique function of the linear speed at the crossover independently of stimulus configuration. However, given the characteristic crossover locations for each stimulus configuration (see Fig. 5), this linear speed is not unique for the 3- and 4-bar stimuli. Some theory is therefore required in order to decide how to average these linear speeds. In addition, one should also consider another non-trivial matter, namely the relative "disambiguating" weights to be associated with the non-crossing (and thus, non-ambiguous) bars in the 3- and 4-bar configurations. In the absence of such a theory, it is reasonable to assume at this point that the "number of bars" effect observed in Fig. 5 can be accounted for in terms of the above factors.

EXPERIMENTS 3–5: REDUCING THE PROBABILITY OF A DISCONTINUITY MATCH

The "crossover" hypothesis predicts that the number of PRs should be proportional to the probability of a discontinuity spatio-temporal match. One obvious way to decrease this probability is to change the relative orientation of the rotating lines: discontinuity matches should not occur for orientation differences beyond the orientation bandwidth of the motion coding mechanisms (about 40 deg according to Gorea & Fiorentini, 1982). This prediction can be easily tested with two rotating bars. Another way of decreasing the probability of a discontinuity match with the 2-bar configuration is to have these bars drawn in opposite polarities. As will be discussed below, however, the interpretation of the opposite-polarity test of the "crossover" hypothesis is complicated by the possibility that such a configuration yields reverse-phi motion (Anstis, 1970).

Finally, a more direct test of the involvement of the crossovers in the instability of a rotating Necker cube is to unstructure the cube so as to decrease the probability of a discontinuity match. Here we report on these three manipulations.*

Method

Stimuli, procedure and observers. There were three stimulus configurations:

1. Two rotating bars of variable relative orientation,
2. Two vertical rotating bars of opposite polarities, and

*Yet other manipulations have been suggested by one of the reviewers. One of these suggestions has actually been implemented and is mentioned in the Discussion section. The remaining ones aim at preventing the occurrence of crossovers (by means of, e.g., blanking the lines just before and after the crossings, increasing the elevation angle).

3. A rotating Necker cube set at different levels of "unstructuring" (see below).

In all cases the length and width of the bars were the same as in the preceding experiments. They rotated as in Experiment 1 around a vertical central axis and were orthogonally projected on the 2D fixation plane at an elevation of 15 deg.

For the two rotating bars of variable relative orientation, one of the bars was always vertical, while the second bar was tilted in such a way as to display an orientation difference from the vertical of 0, 10, 25 and 45 deg at the crossover point. When the two bars were both vertical, this stimulus configuration was identical to the 2-bar condition of Experiment 2, i.e., they occupied the same x,y,z positions as the vertical edges of the rotating Necker cube in Experiment 1. The angular speed could be 25 or 72 turns/min. In the second experimental condition, the two rotating vertical bars were also identical to the 2-bar condition of Experiment 2 with the only difference being their opposite polarities with respect to the 20 cd/m^2 yellow background (contrasts of $\pm 50\%$). Their angular speeds were 25, 40 and 72 turns/min. In the third experimental condition, the unstructured cubes were obtained in two different ways as illustrated in Fig. 6.

One unstructuring procedure consisted of jittering the position of each bar of which the cube was built independently while preserving their orientation (translation jitter). The amount of jitter was characterized by the radius of a sphere in the x,y,z space (see the circles around the vertexes of the cube in Fig. 6); any x,y,z position on the surface of this sphere was equally likely. The unstructuring index (Λ_T) was computed as the ratio between the radius of the sphere, r, and the constant length of the lines, l. In the second unstructuring procedure, the x,y,z location of the bars' barycentres was preserved but their 3D orientation was randomly perturbed. The amount of this orientation jitter was also quantified as the radius of an x,y,z sphere centred on the vertexes of the structured cube and circumscribing the ending of the bars of the unstructured cube around the vertexes. The orientation jitter index, Λ_O, was also given by r/l. It should be noted that, given the random positioning of the bar endings on the surface of the 3D virtual sphere, both Λ_T and Λ_O represent the maximum unstructuring of the cube for a given r. In both cases, the average unstructuring index is given by $\Lambda_T/2$ and by $\Lambda_O/2$.

While the use of the local "deformation sphere" offers a unified metric for the two unstructuring procedures, one should not necessarily expect equal PR rates at $\Lambda_T = \Lambda_O$. A translation jitter of average index $\Lambda_T/2$ (<1) translates into an average bar overlap at the crossover of $1-\Lambda_T/2$ and thus allows for some proportion of spatio-temporal mismatches. On the assumption that the oriented motion detectors are not activated by orientations outside their orientation bandwidth, an average orientation jitter of about 40 deg (i.e., a maximum jitter of 80 deg) should prevent any such mismatches. Given that an average 40 deg orientation jitter translates into an average $\Lambda_O = 0.34$,* the equivalent Λ_T for the translation jitter should still yield a significant amount of spatio-temporal mismatches (i.e., 100%−34% = 66% bar overlap at the crossover).

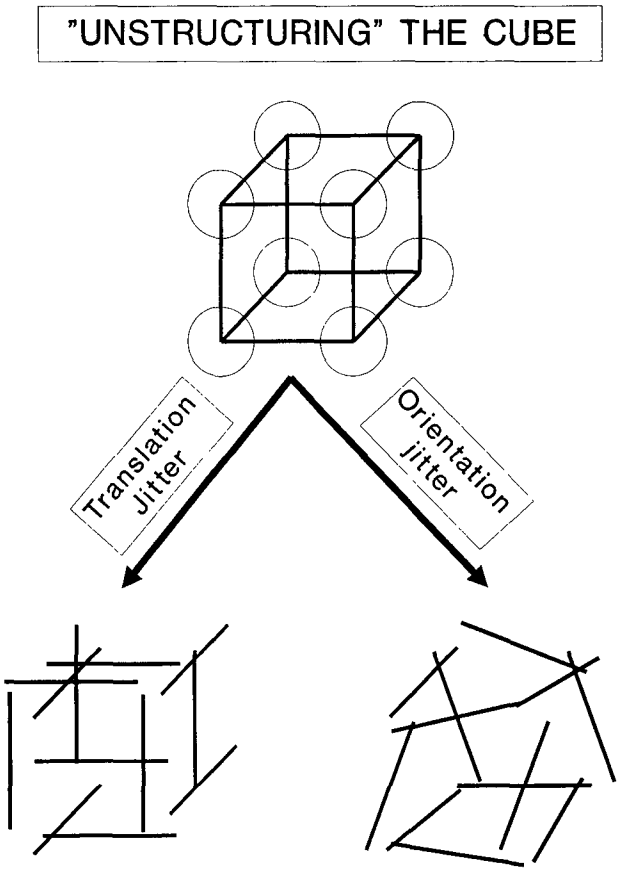

FIGURE 6. Illustration of Necker cube "unstructuring" by means of translation and orientation jitter. The circles centred on the cube's vertexes represent the "deformation spheres" which served as an unstructuring metric for both types of jitter (see text for further details).

Three unstructuring indexes, Λ, were used in this experiment: 0, 0.05 and 0.112. For the orientation jitter, indexes of 0.05 and 0.112 translate into (maximum) angular jitter of 5.74 deg and 12.8 deg, respectively. The structured and unstructured cubes rotated at 25 and 72 turns/min.

The three stimulus configurations described above were run in random order by the same five observers as in Experiment 2. As before, the observers were asked to press a button any time they perceived a rotation reversal. One experimental session (defined by the stimulus configuration, the rotation speed, the relative orientation of the 2-bar stimulus and the unstructuring index) lasted 1 min and was repeated in random order three times. The

*Let r be the radius of the "deformation sphere", l the length of the bars and α the orientation jitter. Then, from the law of cosines, $r^2 = 2(l/2)^2 - 2(l/2)^2\cos(\alpha)$. From this relationship, one finds $\Lambda_T = r/l = 0.34$ for $\alpha = 40$ deg. Conversely, one can find α, given Λ_O from $\alpha = \cos^{-1}(1-2\Lambda_O^2)$.

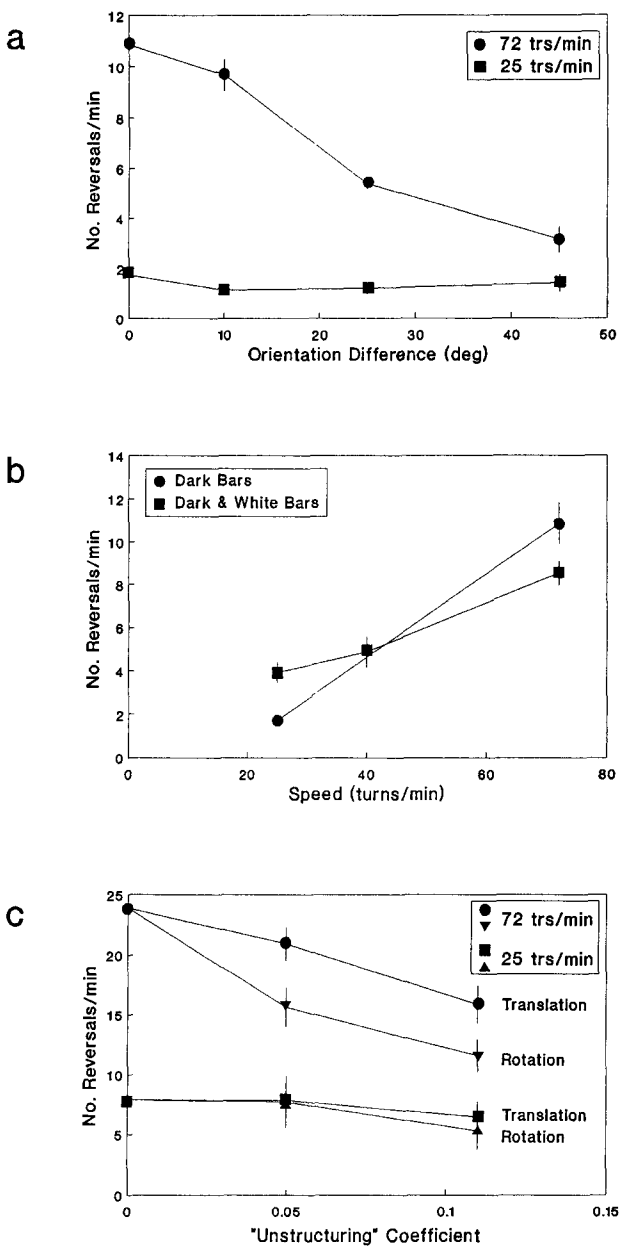

FIGURE 7. PR rates obtained by means of the three stimulus manipulations used in Experiments 3–5: (a) with two bars rotating at 25 (squares) and 72 (circles) turns/min as a function of their relative orientation; (b) with two rotating bars both dark (circles) and of different polarities (squares) as a function of their angular speed; (c) with a cube rotating at 25 (squares and triangles) and 72 (circles and inverted triangles) as a function of its "unstructuring" coefficient (translation jitter: circles and squares; orientation jitter: triangles).

order in which Experiments 2 and 3 were run was also counterbalanced across the five observers.

Results and discussion

Figure 7 displays the number of PRs/min obtained with the two rotating bars of variable orientation (a), of different polarity (b) and with the unstructured cube (c). Each datum point is the PR rate (recorded over a total duration of 3 min) averaged across the five observers. Vertical bars stand for ± 1 SE. The main observations are as follows.

For the two rotating bars of variable orientation [Fig. 7(a)], the PR rate decreases with the orientation difference for 72 turns/min (circles) but not for 25 turns/min (squares). This observation is in perfect accordance with the data of Fig. 1 and with the "crossover" hypothesis which predicts that only high speeds (>25 turns/min) should yield crossover-related PRs. As a consequence, decreasing the efficiency of the crossovers (by increasing the orientation difference) to produce perceptually significant discontinuity speed components (and thus additional PRs) should affect the PR rate yielded by the fast, but not by the slow, stimulus. The PR rate yielded by the latter should be governed only by the ambiguity of its KDE information. It should be noted in this respect that the PR rate observed with the 25 turns/min 2-bar stimulus is about one-third of the PR rate observed with Necker cubes rotating at speeds up to 25 turns/min (see Experiment 1, Fig. 1). This could be an indication that, in comparison with the 2-bar stimulus, the additional bars of the rotating Necker cube reinforce a unitary 3D perception by means of increasing the number of coherent shape-related and KDE-related 3D cues (according to the argument that the absence of 3D perception will, by necessity, entail an absence of PRs). Another possibility is that the additional 3D cues are processed independently and yield therefore independent PRs (see below and the Discussion section). This latter possibility is, however, unlikely for a rigidly rotating object which is perceived as such. In addition, the observation that, for slow rotation speeds, structured and unstructured Necker cubes yield about the same PR rate [see below and Fig. 7(c)] suggests that for such dynamic objects shape information *per se* cannot account for the difference in PR rate between the 2-bar and the Necker cube stimuli. Therefore, the only factor presumably accounting for this difference is the additional KDE information yielded by the latter.

Figure 7(b) shows that the PR rate for both identical (circles) and opposite polarity (squares) rotating bars is an increasing function of speed (above 25 turns/min). However, the main observation corroborating the "crossover" hypothesis is that the slope of this function is significantly smaller (by a factor of about 2) for the opposite polarity bars (0.10) than for the same polarity ones (0.19). Given the reverse-phi phenomenon, one may wonder why the PRs yielded by the opposite polarity bars do increase at all with the rotation speed. One obvious reason is that reverse-phi is not an all-or-none phenomenon in the sense that its strength depends on the relative activation of first- and second-order motion systems, the latter not displaying reversed motion (Chubb & Sperling, 1988; Gorea *et al.*, 1993). In addition, Chubb & Sperling (1989) have shown that, with spatially non-periodic stimuli presented in the fovea (such as those used here), reverse-phi is quite weak or even absent. Other factors such as the non-zero elevation angle of the 2D projections used here yielding strong 3D cues and the fact that bright edges tend to be perceived in front of darker ones (at least at moderate rotation speeds; Dosher *et al.*, 1986) may

also counteract the reverse-phi phenomenon and putatively account for the crossover of the two functions in Fig. 7(b).

Finally, Fig. 7(c) presents the PR rate for unstructured cubes rotating at 25 (squares and triangles) and 72 (circles and inverted triangles) turns/min. For the slow speed, the PR rate is independent of the unstructuring index whether it is manipulated by means of translation (squares) or orientation (triangles) jitter. For the high speed, an increase in the unstructuring index yields a significant decrease in the PR rate for both translation (circles) and orientation (inverted triangles) jitter. As expected (see the Methods section), the orientation jitter is more effective in decreasing the PR rate than the translation jitter. Both observations corroborate, once again, the "crossover" hypothesis: within the slow speed range (up to 25 turns/min) crossovers should not be effective in inducing motion reversals and, as a consequence, unstructuring the cube should not modify the mean PR rate; at high speeds, on the other hand, crossovers should yield additional PRs but an increase of the unstructuring index should decrease their efficiency, the consequence of which is that the overall PR rate should decrease with both translation and orientation jitter.

The data of Fig. 7(c) show that, for the slow speed condition, the PR rate is the same whether or not 2D static shape information is fully available (depending on the unstructuring index). This observation may indicate (other possibilities are addressed in the Discussion section) that shape and KDE information are jointly processed (correlated) at some intermediate stage. Indeed, the rate of PRs should be, in general, positively correlated with the standard deviation of the noise in the system (see the Discussion section). Since the latter presumably increases with the number of independent "3D interpretation sources", the PR rate should be higher when shape and KDE cues are simultaneously present. The particular relationship between PR rate and the number of 3D cues is, however, dependent on a number of specific assumptions. As an example of the difficulty of elaborating on such assumptions, one may note that, at 25 turns/min, the average PR rates for the unstructured cube [Fig. 7(c), squares and triangles] and for the two rotating bars [Fig. 7(a), squares] are about 7 and 1.8, respectively. A possible interpretation of this difference is that the KDE cues for 3D perception are stronger with the unstructured cube than with the two rotating bars; the stronger the (ambiguous) 3D percept, the higher the likelihood that it will reverse. If this were the case, one would need to estimate the relative weights of the shape and KDE cues in 3D perception (see Landy *et al.*, 1995) as a function of the number of visible features/bars. Such an estimation requires further experiments.

GENERAL DISCUSSION

The main results of the present study are as follows.

1. The PR rates yielded by the 2D projection of rotating 3D objects and of a Necker cube in particular, do not depend on their angular speeds up to some critical value (25 turns/min under the specific experimental conditions used here) and increases monotonically with speed thereafter.
2. It is proposed that the function relating PR rate to speed can be accounted for in terms of a form of 2D motion aliasing at the crossover of two or more features (bars) of the rotating 3D object. The motion aliasing hypothesis takes advantage of the following four observations: (i) at the crossover of the rotating elements, there are two, competing, continuity and discontinuity speed components yielding opposite directions; (ii) the discontinuity components cover a spatio-temporal range including both faster (before the crossover) and slower (after the crossover) speeds than the continuity component (see Fig. 2); (iii) relative to the discontinuity components, the continuity component benefits from longer integration periods; (iv) above threshold, effective contrast is a low-pass function of speed. Given these four points, the motion aliasing (or crossover) hypothesis states that, in addition to the inherent ambiguity of the dynamic 2D projection of 3D objects (i.e., the 2D shape and KDE information they yield), perceptual motion/perspective reversals will occur any time the sensitivity to the discontinuity components is critically higher than the sensitivity to the continuity component, namely when the latter is in the range where effective contrast is a decreasing function of speed.
3. The 2D motion aliasing hypothesis was supported by a series of independent experiments where we manipulated the number of crossovers per time unit at a constant speed and the similarity of the crossing bars in terms of their orientation, polarity and spatial overlap. A quantitative formulation of the generalized crossover hypothesis (see Fig. 2) requires, however, more elaborate experiments. In principle, the specification of the interaction range between two drifting objects as a function of their spatio-temporal characteristics should allow one to account for the apparently contradictory reports in the literature on the observed relationship between speed and the bouncing vs crossover percepts yielded by two oscillating bars (Bertenthal *et al.*, 1993; Sekuler *et al.*, 1995). This specification should also provide a way to quantify and predict classical apparent motion phenomena such as those first described by Ternus (passim Koffka, 1935, pp. 299–303) and more recently elaborated upon by Ramachandran & Anstis (1986).

An apparently straightforward prediction of the motion aliasing hypothesis (suggested by one reviewer) is that PRs should always start to increase at the same linear velocity whatever the size of the cube, which is to say, independently of the trajectory length of the bars crossing over. This prediction does not agree with the fact that

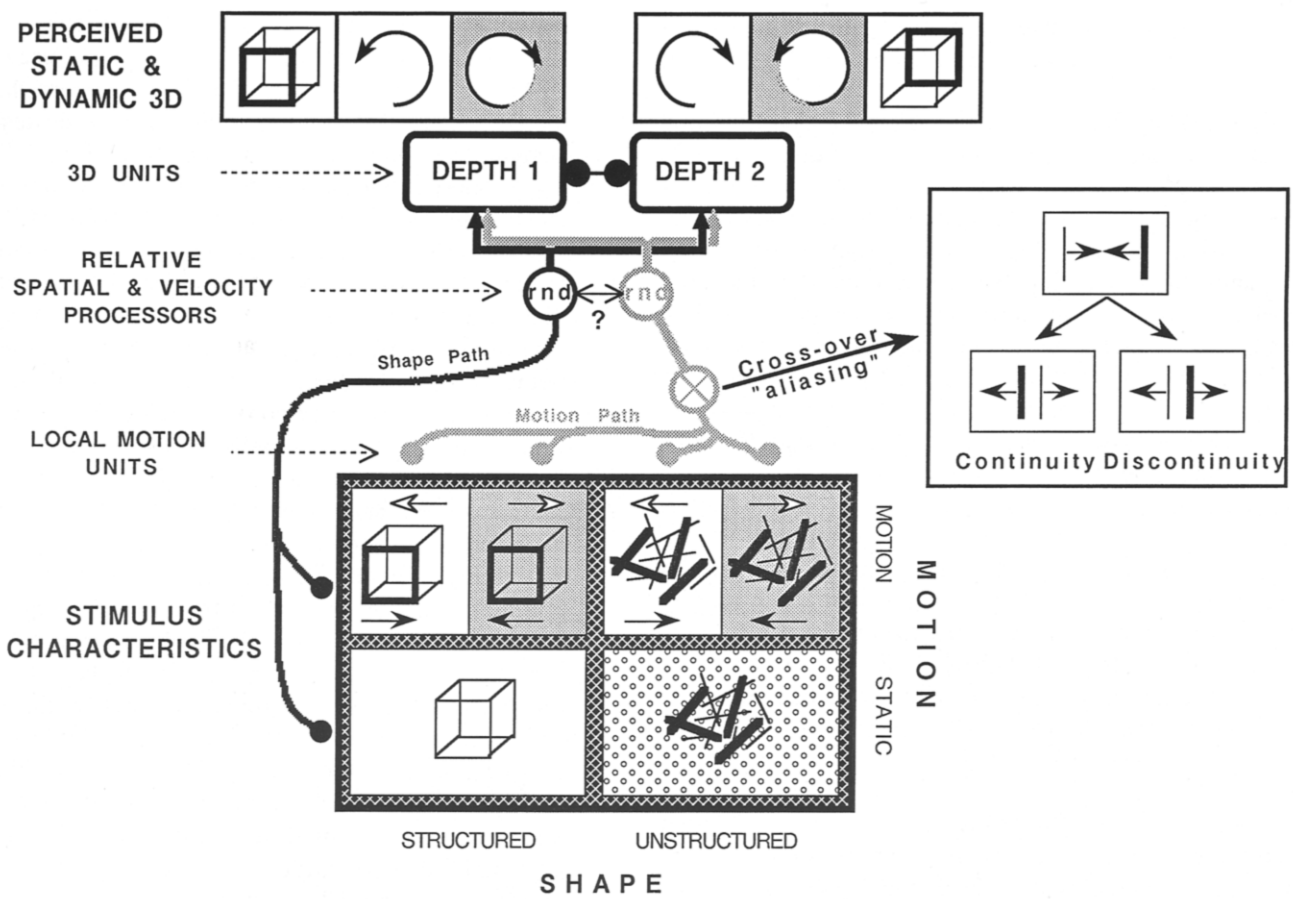

FIGURE 8. Chart illustrating the conjectured Shape and Motion inputs to two exclusive 3D interpretations of an ambiguous 2D image. The bottom, 2×2 entries box (referred to as "Stimulus characteristics") shows the four possibilities of combining 2D Shape (or structure; the horizontal dimension) and 2D Motion information (vertical dimension); the "no structure–no motion" case (small circles in background) does not carry 3D information. White and grey background boxes in the upper part of the "Stimulus characteristics" box and in the "Perceived Static & Dynamic 3D" top row show that the latter are determined by a specific combination of local 2D motion and the current perspective interpretation. See text for further details.

spatio-temporal integration and orientational tuning in space–time (see the *Crossover hypothesis* section) both gain from an increase in trajectory length, thus yielding progressively more activity in the motion sensor responding to the continuity component. On this account, the linear speed at which PRs start increasing should be higher than the corner speed of the effective contrast (and/or sensitivity) function and should increase with trajectory length up to some limit.

Experiments conducted in our laboratory (Agonie, 1996) confirm these predictions. The speed at which two oscillating bars crossing over at fixation appeared to bounce (as opposed to crossover) 50% of the time increased almost linearly from 2.2 to 7.7 deg/sec when their trajectory increased from 1 to 3 deg.* The contrast sensitivity function of speed measured for one of these bars oscillating within a range of 0.4–2 deg was low-pass with a corner velocity of 1 deg/sec or less.

Following the reviewer's suggestion we indirectly replicated this experiment by measuring the PRs as a function of rotation speed with Necker cubes smaller and larger than the one used in the present experiments. For these sizes—1.25, 2.5 and 5 deg of side, the trajectories of the drifting vertical bars are 1.8, 3.5 and 7.1 deg, respectively. The inferred mean linear speeds beyond which PR rate started increasing (NB: a criterion presumably lower than the 50% bouncing used in the two bars experiment) were 1.1, 1.9 and 1.7 deg/sec. Together with the two oscillating bars experiment, these data suggest that the spatial integration limit of the motion sensor optimally responding to a thin drifting bar is somewhere between 1.5 and 1.75 deg, i.e., half of the trajectory length beyond which the critical linear speed yielding additional PRs (or 50% bouncing) remains constant.

*For two oscillating squares, Sekuler *et al.* (1995) (ARVO abstract) report no trajectory effect but the spatial range used is not specified.

The combination of ambiguous 3D sources

From the present experiments one can make a few observations relevant to the issue of how shape and structure-from-motion (or KDE) information is combined to yield an ambiguous interpretation of 3D objects projected in 2D.

The results displayed in Fig. 1 showed that the PR rate is constant (about 4.2 PRs/min) for rotation speeds of 1–25 turns/min. Although we did not collect data for a static

cube, this constancy together with the results presented in the literature (see Kruse & Stadler, 1995) suggest that the PR rate with static and slowly rotating cubes is the same. This observation implies that the combination of shape and KDE, 3D cues is such as to yield the same amount of PRs.

The PR rate observed with two slowly rotating bars [see Fig. 7(a)] which, if static, do not convey any 3D shape information, is significantly smaller than the PR rate yielded by either the structured (Fig. 1) or the unstructured [Fig. 7(c)], slowly rotating cube. Taken together, these observations suggest that the higher PR rate observed with the more complex rotating objects is not due to the summation of shape and KDE cues but rather to the additional KDE (and therefore 3D) cues they yield relative to the 2-bar stimulus. Obviously, this line of reasoning requires further experiments to show that it holds, even for "unstructuring" indexes higher than those used in these experiments (i.e., a maximum of 11.2%).

Standard models of perceptual instability (see Kruse & Stadler, 1995) and, in particular, of the bistability yielded by a Necker cube (e.g. Lehky, 1995; Maloney & Gorea, 1995) agree in that the observed bistability is a pure random (Poisson) process triggered by the noise in the system (presumably limited to some extent by an exponentially decaying refractory/inhibitory period; but see Maloney & Gorea, 1995). If a rotating Necker cube involves two independent, equal variance noise sources (i.e., from an independent processing of static 2D-shape and of KDE), given that a static Necker cube yields about 4 PRs/min and assuming that the time-base (internal clock) of the random process is in the range of 10 (or 100) msec, it can be shown that a rotating Necker cube should yield about 70 (or 24) PRs/min (see Appendix). Clearly, the present data do not show such a trend, at least for slow angular speeds. The most obvious account of this discrepancy between data and predictions is that static 2D-shape and KDE are not independent (ambiguous) sources to the 3D processing units. There are other possibilities.

As already noted, the possibility exists that the KDE source of 3D information is actually the probabilistic sum of several, more local, independent processes which would account for the increase in PR rate when the number of rotating bars increases from 2 [Fig. 7(a, b) to 12 [Fig. 1 and Fig. 7(c)]. If this were the case, the addition of the 2D shape source would increase the standard deviation of the overall bistable process by a small, unnoticeable amount and, in line with the argument above, would yield a negligible increase in the PR rate. A second possibility is that the noise of the two sources of ambiguity is not Gaussian. No prediction concerning the variation in PR could then be made. Future experiments might come to support one of these possibilities.

Figure 8 is presented here as a tentative conclusion of this study. 2D Shape/Structure and 2D Motion inputs (the horizontal and vertical dimensions of the bottom box, respectively) are randomly fed (dark and grey paths in the chart) into either one of two exclusive (i.e., reciprocally inhibitory) 3D interpretations (boxes "Depth 1" and "Depth 2") after connecting to intermediate stages (circles) where relative position and speed relationships are computed. The outputs of these intermediate processing stages are, from the standpoint of their 3D interpretation, inherently ambiguous and are therefore randomly fed into one of the two 3D-boxes. In the process of computing motion, motion aliasing occurs within some critical spatio-temporal range before the KDE processing stage (the box on the right-hand side of the chart). These 2D motion interactions yield additional ambiguous 2D information. The shape and motion pathways may be regarded as independent (as drawn) or as having correlated outputs (double arrow and question mark between the two "rnd" circles). In any case, depending on the current 3D interpretation (i.e., perceived perspective) and on the local 2D motion direction, 3D motion will be perceived as clockwise or counterclockwise (top boxes). Also, any reversal of the perceived 2D direction due to motion aliasing at the crossover will yield a rotation reversal. When both local 2D motion direction and perspective are simultaneously reversed (a very unlikely event), the overall 3D perception will remain unchanged. Thus, 3D interpretations are directly related to the 2D spatio-temporal structure of the stimulus.

REFERENCES

Agonie, C. (1996). L'instabilité perceptive étudiée avec le cube de Necker. Ph.D. Thesis, E.H.E.S.S., Paris France.

Anstis, S. (1970). Phi movement as a subtraction process. *Vision Research, 10*, 1411–1430.

Bertenthal, B. I., Banton, T. & Bradbury, A. (1993). Directional bias in the perception of translating patterns. *Perception, 22*, 193–207.

Burr, D. C. & Ross, J. (1982). Contrast sensitivity at high velocities. *Vision Research, 22*, 479–484.

Chubb, C. & Sperling, G. (1988). Drift-balanced random stimuli: a general basis for studying non-Fourier motion perception. *Journal of the Optical Society of America A, 5*, 1986–2007.

Chubb, C. & Sperling, G. (1989). Two motion perception mechanisms revealed by distance driven reversal of apparent motion. *Proceedings of the National Academy of Sciences USA, 86*, 2985–2989.

Dosher, B. A., Sperling, G. & Wurst, S. A. (1986). Tradeoffs between stereopsis and proximity luminance covariance as determinants of perceived 3D structure. *Vision Research, 26*, 973–990.

Flamm, L. E. & Bergum, B. O. (1977). Reversible perspective figures and eye movements. *Perceptual and Motor Skills, 44*, 1015–1019.

Gale, A. G. & Findlay, J. M. (1983). Eye movement patterns in viewing ambiguous figures. In Groner, R., Menz, C., Fisher, D. F. & Monty, R. A. (Eds), *Eye movements and psychological functions: International views* (pp. 145–168). Hillsdale, NJ: Lawrence Erlbaum.

Georgeson, M. A. & Sullivan, G. D. (1975). Contrast constancy: deblurring in human vision by spatial frequency channels. *Journal of Physiology, London, 252*, 627–656.

Gorea, A. & Fiorentini, A. (1982). Interactions orientationnelles entre des réseaux stationnaires et en mouvement. *L'Année Psychologique, 82*, 45–65.

Gorea, A. & Lorenceau, J. (1984). Perceptual bistability with counterphase gratings. *Vision Research, 24*, 1321–1331.

Gorea, A., Papathomas, T. V. & Kovacs, I. (1993). Motion perception with spatio-temporally matched chromatic and achromatic information reveals a "slow" and a "fast" motion system. *Vision Research, 33*, 2515–2534.

Kelly, D. H. (1979). Motion and vision. II. Stabilized spatio-temporal

threshold surface. *Journal of the Optical Society of America, 69*, 1340–1349.
Koffka, K. (1935). *Principles of Gestalt psychology*. Routledge & Kegan Paul: London.
Kruse, P. & Stadler, M. (Eds) (1995). *Ambiguity in mind and nature*. Berlin: Springer.
Kulikowski, J. J. (1976). Effective contrast constancy and linearity of contrast sensation. *Vision Research, 16*, 1419–1431.
Landy, M. S., Maloney, L. T., Johnston, E. B. & Young, M. (1995). Measurement and modeling of depth cue combination: in defense of weak fusion. *Vision Research, 35*, 389–412.
Lehky, S. R. (1995). Binocular rivalry is not chaotic. *Proceedings of the Royal Society of London B, 259*, 71–76.
Maloney, L. & Gorea, A. (1995). A model of bi-stable perception of a Necker cube. *Perception Supplement, 24*, 31.
McKee, S. P. & Welch, L. (1985). Sequential recruitment in the discrimination of velocity. *Journal of the Optical Society of America A, 2*, 243–251.
Ramachandran, V. S. & Anstis, S. M. (1986). The perception of apparent motion. *Scientific American, 2546*, 80–87.
Sabrin, H. W. & Kertesz, A. E. (1983). The effect of imposed fixational eye movements on binocular rivalry. *Perception & Psychophysics, 34*, 155–157.
Sekuler, R., Sekuler, A. B. & Brackett, T. (1995). When visual objects collide: repulsion and streaming. *Investigative Ophthalmology and Visual Science, Supplement, 36*, S50.
Todd, J. T. & Norman, J. F. (1995). The effects of spatio-temporal integration on maximum displacement thresholds for the detection of coherent motion. *Vision Research, 35*, 2287–2302.
Watson, A. B. & Ahumada, A. J. (1983). A look at motion in the frequency domain. NASA Technical Memo TM-84352.

Acknowledgements—We thank Larry Maloney and Jean-Didier Bagot for the many helpful discussions we have had while this work was in progress. Parts of the present studies have been reported at the Association for Vision Research and Ophthalmology, Fort Lauderdale, Florida, 1995 and at the 18th European Conference on Visual Perception, Tübingen, 1995. This work was supported by a DRET scholarship to C. Agonie and by grant PRET 94-047 to A. Gorea.

APPENDIX*

If perceptual bistability yielded by a Necker cube is governed by a pure Poisson process mirroring a Gaussian noise in the system, the standard deviation, σ_2, of the sum of two independent, equal variance Gaussian noise sources (like static 2D-shape and KDE) should be $\sqrt{2}$ larger than the standard deviation of each of them, σ_1. A PR will be observed any time the noise exceeds some criterion β.† The ratio, $R(\beta)$, between the probability of one source and the probability of two independent sources of exceeding β is then given by:

$$R(\beta) = \frac{1 - \int_{-\infty}^{\beta} \frac{1}{\sigma_1\sqrt{2\pi}} e^{-x^2/2\sigma_1^2} dx}{1 - \int_{-\infty}^{\beta} \frac{1}{\sigma_2\sqrt{2\pi}} e^{-x^2/2\sigma_1^2} dx}$$

The function $R(\beta)$ is shown in Fig. A1. When the criterion is zero (which is to say that an infinitesimal difference between the activation of the bistable states will trigger a PR), $R = 1$, an intuitive result. As β increases, the σ_2 process is progressively more likely to exceed that criterion than the σ_1 process. When the criterion β is set at about 2.2 times σ_1 (which is unknown), a double-source bistable process will yield five times more PRs than a single-source unstable process.

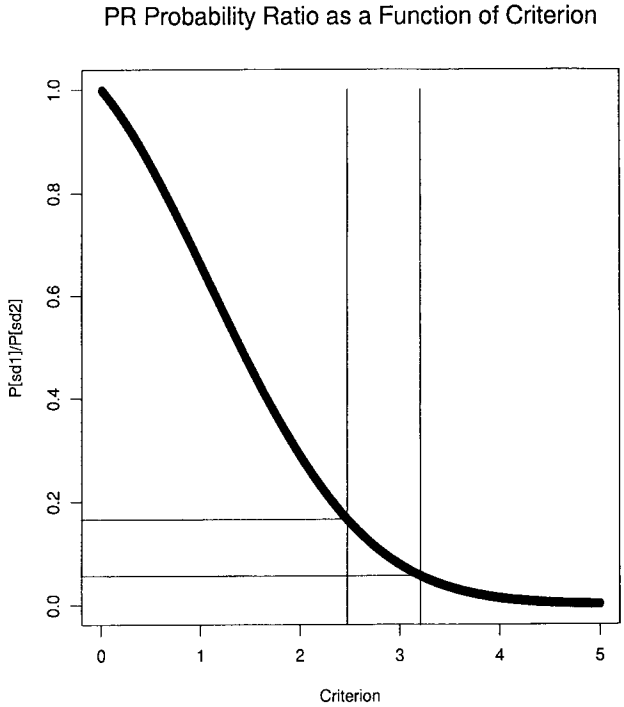

FIGURE A1. The ratio of the probabilities of exceeding the criterion β of two random, Gaussian variables, one of which (the denominator) has a standard deviation $\sqrt{2}$ larger than the other. The vertical lines show two such criteria, 2.47 and 3.21 σ-units, computed on the assumption that the neural sampling rate is 100 and 10 msec, respectively, and given that the observed average PR rate at slow speeds is 4 turns/min.

One may attempt to speculate on the precise criterion used by the visual system as follows. A static (or slowly rotating) Necker cube yields, on average, 4 PRs/min. If the criterion β is set at 0, a binary random variable would yield, on average, a reversal every two draws, i.e., a PR probability for each draw of $p = 0.5$. It follows that the time-base of the random process (the "internal clock") should be 60 sec/(2×4), i.e., 7.5 sec. This is a highly unlikely time-base for a neural system whose response time is rather within the range of milliseconds. If the time-base is set at 10 msec, there will be 6000 draws/min and the probability of exceeding the criterion β required to yield 4 PRs/min will be 4/6000 = 0.00066. The criterion β is then given as the $z(0.00066)$ score, namely 3.21. If the time-base of the system is 100 msec, the criterion β yielding an average of 4 PRs/min is 2.47. These two β-values are shown as vertical lines in Fig. A1. For these criteria, the double-source bistable process will yield, respectively, 17.5 and 6 times more PRs than the single-source process.

*This section was developed in collaboration with Larry Maloney.
†The criterion β can be related to the stability of a dynamic system. Technically, it refers to the depths of the wells of the potential function governing the system. It is assumed here that this stability (or β) is invariant with the number 3D sources.